Cathodic Behavior of Titanium Diboride in Aluminum Electrolysis

B. Mazza, G. Serravalle, G. Fumagalli, and F. Brunella

Dipartimento di Chimica Fisica Applicata, Politecnico di Milano, 20133 Milano, Italy

ABSTRACT

The results of a laboratory investigation concerning the cathodic behavior of TiB_2-based materials in aluminum electrolysis are presented and discussed. X-ray microanalysis reveals sodium penetration, the extent of which is in agreement with electrochemical predictions considering the codeposition of sodium with the aluminum at the cathode.

The application to cathode design of conductive materials wetted by liquid aluminum [*e.g.*, titanium diboride and other similar materials often referred to as refractory hard metals (RHM)] represents the most promising medium-term modification for reducing energy usage in the conventional Hall-Héroult process (1-9). The cell would then be operated with a thin film of liquid metal on the sloped bottom, avoiding the detrimental effects due to electromagnetic agitation, and the anode-cathode distance could therefore be reduced significantly along with the cell voltage. Thus, the values of the specific energy consumption attainable would lie in the range of 10 ÷ 11 kWh/kgAl, instead of the about 13 kWh/kgAl presently being obtained in the most advanced cells (with high amperage, computer control of cell operation, and continuous alumina feeding, as well as control of magnetic effects).

The operation of a TiB_2 cathode cell, whatever its design, will lead to a situation substantially different from that of a conventional cell, with possible adverse effects on current efficiency, concentration polarization, decomposition voltage of alumina, anode gas bubble behavior, alumina dissolution, and heat balance. In previous papers (10-12), a theoretical analysis of the above aspects was accomplished outlining the main problems in view of their experimental closer study. On the other hand, as to the electrochemical aspects only, a better understanding of the cathodic reaction phenomena attainable through laboratory tests would be of basic importance to predict the performance of an industrial cell with TiB_2-based cathodes. Within the frame of reference sketched out above, this paper presents and discusses the results of a laboratory investigation concerning the cathodic behavior of TiB_2-based materials in aluminum electrolysis and the chemical effect of sodium codeposition on the cathode material.

Experimental

Materials.—The commercial TiB_2-based materials used as cathodes are briefly described and characterized in Table I. The overall characterization[1] included chemical composition, microstructure, physical and mechanical properties, and chemical resistance to oxidation in air and to corrosion in molten aluminum and cryolite-alumina melts (13). Graphite (Union Carbide Corporation, grade ATJ) was also used for comparison. All the experiments were performed with small disks having 25 mm diameter and 5 mm thickness.

[1] Performed within the same research project at the University of Padova.

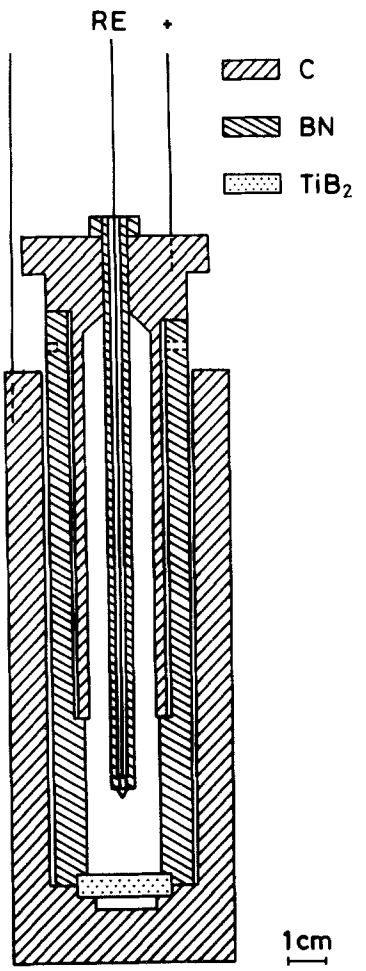

Fig. 1. Miniature electrolysis cell (RE stands for reference electrode)

Electrochemical measurements.—The miniature cell used for cathodic polarization measurements in cryolite-alumina melts is shown in Fig. 1. The reference electrode was a graphite one, which, after a suitable anodic prepolarization, exhibited a potential stable to ±5 mV.

Table I. Characterization of the commercial TiB_2-based materials used as cathodes (13)

RHM material	Manufacturer	Main constituents[a]	Density[b] (g/cm³)	Electrical resistivity[b] (μΩ cm)	Thermal expansion coefficient[c] (1/°C)
RHM 1	Carborundum Co.	TiB_2, AlB_2, AlN	3.96	62	8×10^{-6}
RHM 2	Borax Consolidated Ltd.	TiB_2, AlN, BN	3.23	1520	7.3×10^{-6}

[a] Identified by x-ray diffraction.
[b] At 20°C.
[c] Temperature range: from 20° to 990°C.

For comparison, the following properties for pure TiB_2 manufactured by Norton Company are given: density 4.45 g/cm³ (≃ 99% of theoretical value), electrical resistivity 9.5 μΩ cm, thermal expansion coefficient 8.9×10^{-6}/°C.

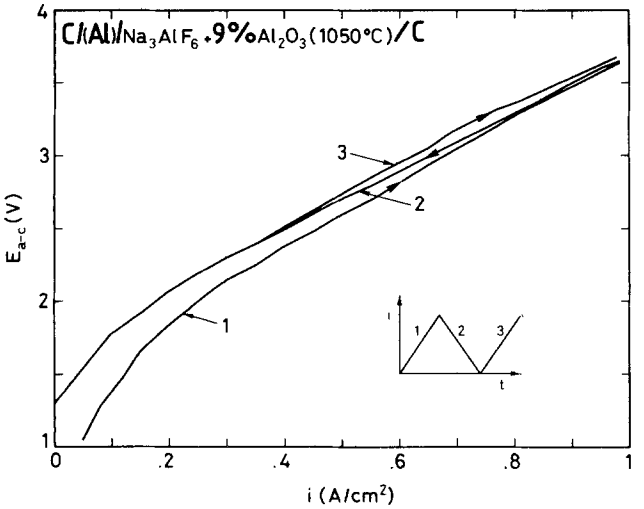

Fig. 2. Determination of cathodic polarization curves by means of the cyclic amperodynamic method (for simplicity, the potential difference between anode and cathode, $E_{a\text{-}c}$, was recorded in this test).

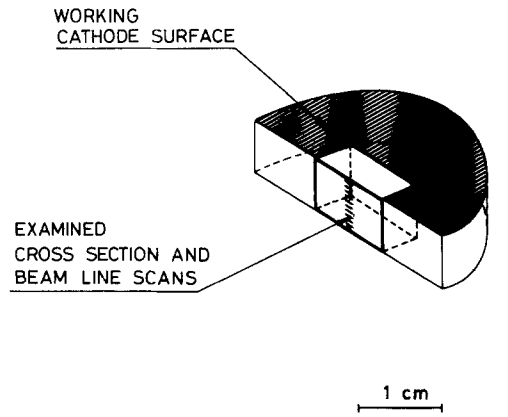

Fig. 4. Explanatory sketch for specimen cutting from the cathode and examining in the electron microprobe analyzer.

As is well known (14), graphite electrodes dipping into cryolite-based melts are of common use as a reference due to their simplicity, in spite of a nonthorough comprehension of the electrode processes taking place on them. The cell was placed in the isothermal zone of a wire-wound resistance furnace, under a nitrogen continuous flow. The temperature was controlled at 1050° ± 5°C. This value is somewhat higher than the operating temperature for industrial reduction cells (around 960°C), and it was selected to make the available range of melt compositions wider.

In order to attain a better reproducibility of results, the standardization of polarization measurements pointed out the necessity of limiting their duration in time and, on the other hand, of operating after a thin film of aluminum had covered the cathode because of current circulation: a cyclic amperodynamic technique was therefore employed (see current/time function in Fig. 2). A remarkable difference was observed (Fig. 2, curves 1 and 2) between the potential responses recorded during the first two current sweeps, in the forward and reverse direction, respectively, starting from an open circuit in the absence of aluminum on the cathode. However, when successively repeating current sweeps, the potential responses differed only slightly (see Fig. 2, curves 2 and 3). As a rule, only the first two current sweeps were developed (at a sweep rate of 0.3 mA/cm²s and with a sweep reversal current density of 0.7 A/cm²) and the second (reverse) sweep was taken into account, with a slow recording of the potential difference between reference electrode and cathode.

The ohmic drop error in the measured cathode potential could not reliably be corrected by calculation. Therefore, it was necessary to determine it experimentally through a galvanostatic pulse technique, with fast (oscillographic) recording of the potential decay at the current switch-off (Fig. 3). The above ohmic drop determination was carried out both before and after the cyclic amperodynamic experiments.

Current/time functions were applied using an Amel Type 555 B potentiostat/galvanostat with an Amel Type 567 function generator. The potential/current or potential/time responses were recorded on an Amel Type 868 Y-t recorder, or on a Gould Y-t oscillographic recorder.

X-ray microanalyses.—Cathode samples were analyzed using a Cameca Camebax electron beam microprobe with wavelength dispersive x-ray spectrometer. The characteristic K_α x-ray lines for sodium and fluorine were detected under the following operating conditions: accelerating potential 15 kV, specimen current about 60 nA, tilted spectrometer with a thallium acid phthalate crystal, gas flow proportional counter with a mixture of argon and methane as flowing gas, and counting time 50s.

Specimens were cut out from cathodes, as shown in Fig. 4, and were then embedded in synthetic resin, ground with emery papers to a 800 mesh finish and metallized with carbon. Beam line scans of approximately 1 mm in length (observation at 2000 times magnification)

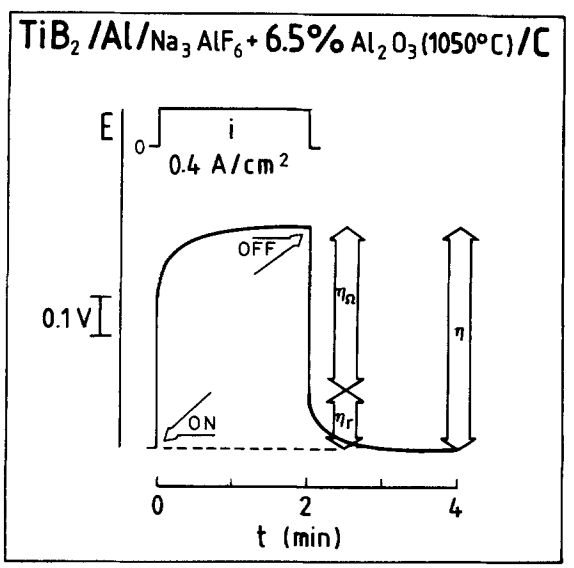

Fig. 3. Oscillographic recording of the cathode potential, E, showing the ohmic drop determination by means of the galvanostatic pulse method (η is the "apparent" cathode overvoltage, η_Ω the ohmic voltage drop, η_r the "residual" cathode overvoltage).

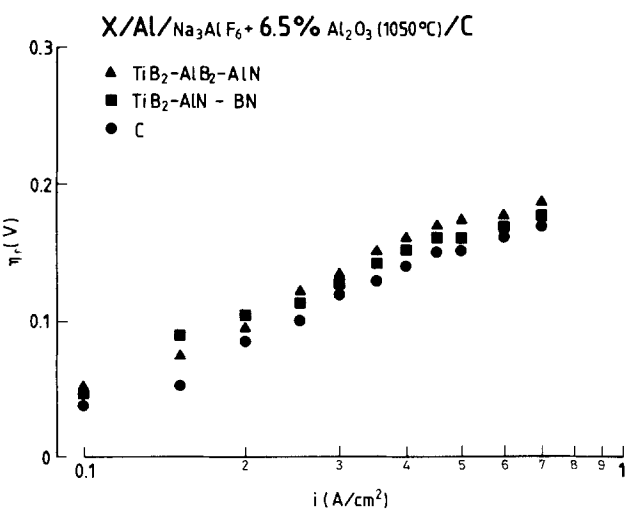

Fig. 5. Cathodic polarization curves for two different RHM materials (RHM 1 and RHM 2, see Table I) and graphite.

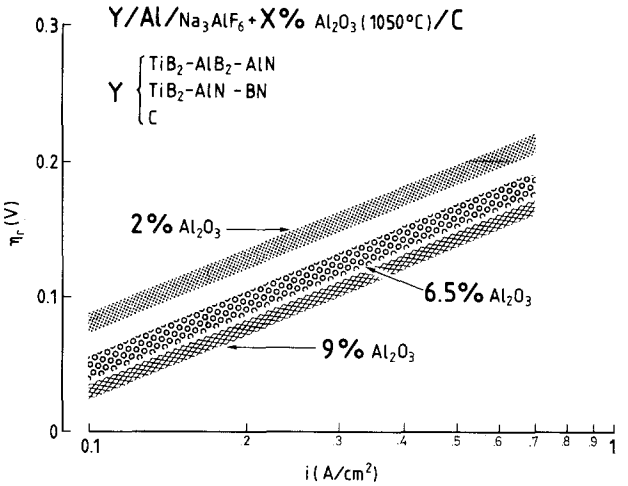

Fig. 6. Cathodic polarization curves for different values of alumina content in the bath, regardless of the cathode material (RHM 1, RHM 2 or graphite). (All the percentage compositions are in weight percent.)

and parallel to the cathode surface were successively repeated on the cross section surface at depth intervals of 10 μm (see Fig. 4) in order to obtain penetration profiles for the considered elements. The aforesaid scan length value was chosen so as to obtain the x-ray signals from a sufficiently large sample volume, thus minimizing the effects of heterogeneities on a microscopic scale, such as surface microroughness[2] and grain boundaries.

Results were expressed in terms of the ratio between the x-ray peak intensity for each element measured on cathode sample[3] and the peak intensity measured on an elemental standard (a glass of known composition containing Na_2O and marked 60306 for sodium, and a CaF_2 crystal for fluorine). The intensity values for cathode samples were corrected for background by subtracting the values measured on a sample that had never worked as cathode.

It is necessary to point out that the conversion of x-ray intensity data to chemical composition (sodium and fluorine percentages) could not be made owing to the inaccuracies and uncertainties involved by the analysis of light elements (standards of nearly the same composition as the specimen were obviously not available). Nevertheless, the experimentally collected data were comparable one with another.

[2] The tilted spectrometer, too, was used for counteracting this effect.

[3] At any penetration depth.

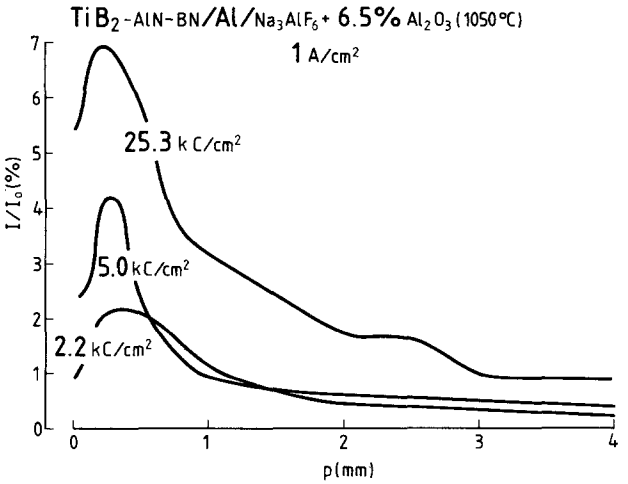

Fig. 7. Sodium penetration profiles inside the RHM 2 cathode material for different values of specific charge (I/I_0 is the ratio between the net intensity of x-rays emitted by the cathode material and that emitted by a standard; p is the penetration distance from the working cathode surface, see Fig. 4).

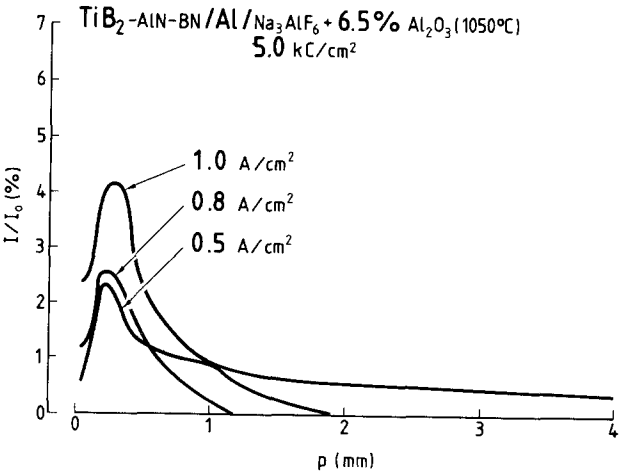

Fig. 8. Sodium penetration profiles inside the RHM 2 cathode material for different values of current density.

Results and Discussion

Figure 5 shows that, regardless of the cathode material (RHM 1, RHM 2, or graphite), the overvoltage results (corrected for ohmic drop) are quite similar; the semilogarithmic plots *vs.* current density are straight over a wide range, with a slope of about 0.16 V/decade. As far as the other variables are concerned, the influence of the bath alumina content overcomes the scatter due to the effect of the cathode material: the overvoltage rises only slightly when the alumina content decreases from 9 to 5%, but it significantly grows when the same content diminishes to about 2% (Fig. 6).

In conclusion, in comparison with the conventional graphite, TiB_2-based materials do not considerably modify the cathode phenomena provided that a thin film of liquid aluminum is deposited. On the one hand, the charge transfer overvoltage on the liquid aluminum cathode is commonly recognized (15, 16) to be negligible at normal current densities; on the other hand, the existence of an appreciable concentration overvoltage is well known, too (15, 16), which is caused by the concentration gradients set up in the electrolyte layer adjacent to the cathode, with aluminum donor depletion and sodium ion enrichment leading to the simultaneous separation of sodium.[4]

With the view of a closer study of the sodium deposition and its effects,[5] besides electrochemical tech-

[4] In the conventional industrial cells at normal operational conditions, this effect is substantially reduced, since the concentration of aluminum donors is sufficiently high and the electromagnetic agitation homogenizes the melt, thus minimizing the concentration overvoltage.

[5] As is well known (17-19), sodium penetration (besides electrolyte penetration) into the cathode carbon with formation of intercalation compounds appears to be the main reason for the aging of the cathode lining in industrial cells.

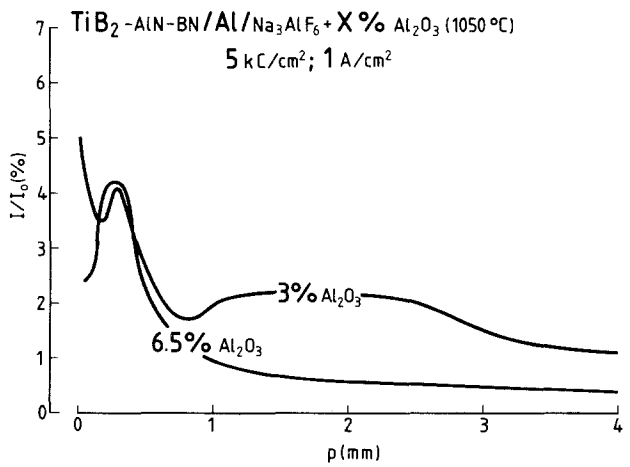

Fig. 9. Sodium penetration profiles inside the RHM 2 cathode material for different values of alumina content in the bath.

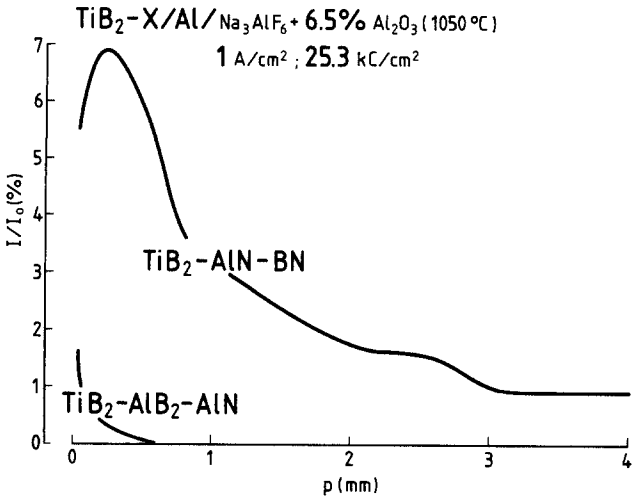

Fig. 10. Sodium penetration profiles inside two different RHM cathode materials (RHM 1 and RHM 2).

niques, x-ray microanalysis techniques were applied to quantify the chemical changes occurring in TiB_2-based materials and caused by cathodic operation. The results of this investigation show an increase of the level and penetration depth of sodium within the RHM 2 cathode material at the increase of the specific charge (Fig. 7) or current density (Fig. 8) and at the decrease of the alumina content in the bath (Fig. 9), in agreement with electrochemical predictions. On the other hand, the absence of fluorine[6] within the cathode material was recorded for depths of more than about 100 μm from the electrode surface [which means beyond an equivalent thickness of material penetrated with the cryolite bath (as shown by a sodium-to-fluorine molar ratio resulting that is stoichiometrically consistent)].[7]

As to the influence of the material, the described sodium penetration phenomenon after cathodic operation is significantly more marked for the RHM 2 than for the RHM 1 material (Fig. 10). In this connection, the microscopic observation of the cross sections of the two cathodes after removal from the electrolysis cell pointed out (Fig. 11) how the RHM 1 material may easily be covered by a continuous film of liquid aluminum, where the solubility of gaseous sodium at around 1000°C is very low, *i.e.*, about 0.13 weight percent at 1 atm sodium pressure (20, 21). The contrary occurs for the RHM 2 material on which aluminum droplets are present, thereby rendering the deposition of sodium possible on wide areas directly in contact with the bath.[8] What above might explain the different behavior of the two materials. The poor wetting of the Al/RHM 2 system is to be ascribed to the presence of the BN constituent, which, as is well known, is not wetted by liquid aluminum.[9] This also results in a higher resistance to molten aluminum (being the contact less intimate); for example, weight loss measurements[10] after a 200h exposure to metal pad in an industrial cell gave values of about 0.30% of the initial weight for the RHM 2 material and 0.40% for RHM 1 (23).

In order to determine the sodium distribution among the different constituents of the RHM 2 cathode material, the characteristic K_α x-ray line traces for sodium and titanium were made[11] in the zone of TiB_2 grains. An expressive example is shown in Fig. 12: there was no sodium in the interior of the TiB_2 grains. This result is con-

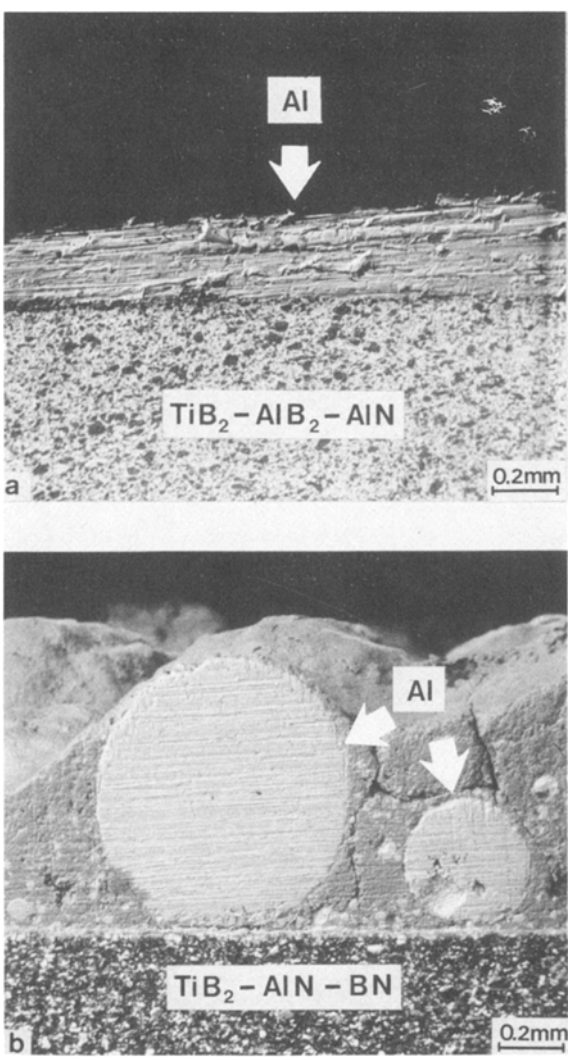

Fig. 11. Photomicrographs showing the interface region of electrode/electrolyte (cross section) for two different RHM cathode materials (RHM 1 and RHM 2) after removal from the electrolysis cell.

[6] Below the minimum detectability limit of the apparatus.

[7] Sodium penetration data reported in Fig. 7-10 were corrected for this contribution arising from the electrolyte penetration.

[8] A similar situation is faced during the initial period of electrolysis in industrial cells, when the most intensive sodium penetration into the carbon cathode lining occurs.

[9] Also, the Al/AlN system exhibits less wetting than the Al/TiB_2 system (22).

[10] Performed within the same research project at the Aluminia S.p.A. Portoscuso Works.

[11] Under the following operating conditions: accelerating potential 10 kV, specimen current about 100 nA, tilted spectrometer with thallium acid phthalate and pentaerythritol crystals for sodium and titanium, respectively.

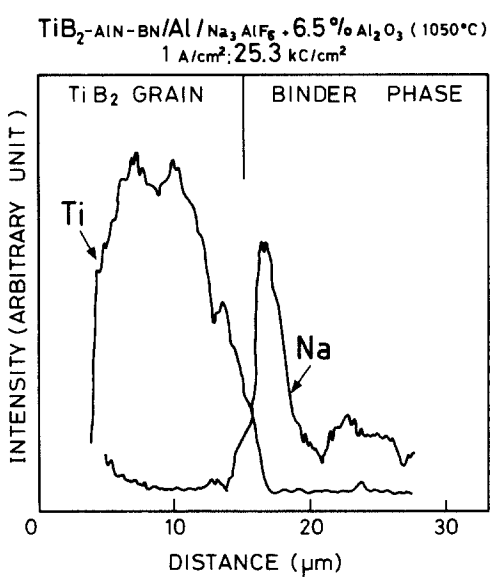

Fig. 12. Distribution of sodium and titanium across the interface of TiB_2 grain/binder phase for the RHM 2 cathode material, at a depth from the cathode surface of 300 μm (corresponding to the maximum of the sodium penetration profile inside the material considered, see Fig. 10).

sistent with the evidence, reported in other studies, of the attack of liquid sodium at grain boundaries of Si_3N_4 and Sialon ceramics (24) and of intergranular aluminum penetration of TiB_2 (about 96% dense) used as a cathode in aluminum reduction cells (25).

Conclusions

X-ray microanalysis of TiB_2-based materials after cathodic operation in aluminum electrolysis reveals sodium penetration, the extent of which is in agreement with electrochemical predictions considering the codeposition of sodium with the aluminum. A remarkable influence of the material is to be ascribed to its wettability by liquid aluminum. Sodium penetration does not occur in the interior of the TiB_2 grains but at the grain boundary.

Acknowledgments

This research was supported by the Consiglio Nazionale delle Ricerche within the Progetto Finalizzato Metallurgia. The authors are grateful to D. Manno for the assistance in the electrochemical measurements, and to M. Verità and R. Basso for their cooperation and support in the x-ray microanalyses performed at the Stazione Sperimentale del Vetro, Venezia-Murano.

Manuscript submitted June 19, 1986; revised manuscript received Sept. 22, 1986.

The Dipartimento di Chimica Fisica Applicata, Politecnico di Milano assisted in meeting the publication costs of this article.

REFERENCES

1. K. Billehaug and H. A. Øye, *Aluminium*, **56,** 642 (1980); *ibid.*, **56,** 713 (1980).
2. J. B. Todd, *J. Met.*, **33,** 42 (1981).
3. T. R. Beck, in "Electrochemistry in Industry, New Directions," U. Landau, E. Yeager, and D. Kortan, Editors, p. 331, Plenum Press, New York (1982).
4. R. C. Dorward, *J. Appl. Electrochem.*, **13,** 569 (1983).
5. K. J. Brondyke, *J. Met.*, **35,** 63 (1983).
6. J. W. Evans, in "Extended Abstracts of the 35th ISE Meeting," p. 748, Berkeley, California (1984).
7. L. G. Boxall, A. V. Cook, and H. W. Hayden, *J. Met.*, **36,** 35 (1984).
8. P. Duby, *ibid.*, **37,** 63 (1985).
9. R. C. Dorward and J. R. Payne, Reports to Department of Energy for Contract DE-ACO3-76CS40215, Kaiser Aluminum and Chemical Corp., Pleasanton, California.
10. A. Bonfiglioli, F. Gregu, G. Serravalle, B. Mazza, G. Fumagalli, D. Festa, and R. Dal Maschio, *Metall. Ital.*, **75,** 194 (1983); *ibid.*, **75,** 259 (1983).
11. G. Degan, G. Fumagalli, F. Gregu, B. Mazza, and G. Serravalle, in "Proceedings of the 84th Riunione Annuale Associazione Elettrotecnica ed Elettronica Italiana, Cagliari, Italy," Vol. 58, Paper A.31, AEI, Milano (1983).
12. B. Mazza, A. Bonfiglioli, F. Gregu, and G. Serravalle, *Aluminium*, **60,** 740 (1984).
13. D. Festa, in "Proceedings Convegno Conclusivo Progetto Finalizzato Metallurgia, Terni, Italy," Vol. 1, p. 1163, CNR, Roma (1985).
14. K. Grjotheim, C. Krohn, M. Malinovsky, K. Matiasovsky, and J. Thonstad, "Aluminium Electrolysis, The Chemistry of the Hall-Héroult Process," Chap. 6, Aluminium-Verlag GmbH, Düsseldorf (1977).
15. R. Piontelli, B. Mazza, and P. Pedeferri, *Electrochim. Metall.*, **1,** 217 (1966).
16. J. Thonstad and S. Rolseth, *Electrochim. Acta*, **23,** 223 (1978); *ibid.*, **23,** 233 (1978).
17. K. Grjotheim and B. J. Welch, "Aluminium Smelter Technology, A Pure and Applied Approach," Chap. 5, Aluminium-Verlag GmbH, Düsseldorf (1980); K. Grjotheim, C. Krohn, M. Malinovsky, K. Matiasovsky, and J. Thonstad, "Aluminium Electrolysis, The Chemistry of the Hall-Héroult Process," p. 330, Aluminium-Verlag GmbH, Düsseldorf (1977).
18. B. Panebianco and R. Bacchiega, *Alluminio*, **35,** 69 (1966).
19. H. Latreille, *Electrochim. Metall.*, **4,** 111 (1969).
20. W. Jander and H. Herrmann, *Z. Anorg. Allg. Chem.*, **239,** 65 (1938).
21. C. E. Ransley and H. Neufeld, *J. Inst. Met.*, **78,** 25 (1950).
22. S. K. Rhee, *J. Am. Ceram. Soc.*, **53,** 386 (1970).
23. V. Bellò, in "Proceedings Convegno Conclusivo Progetto Finalizzato Metallurgia, Terni, Italy," Vol. 1, p. 1151, CNR, Roma (1985).
24. R. N. Singh and W. D. Tuohig, *J. Am. Ceram. Soc.*, **58,** 70 (1975).
25. R. C. Dorward, *ibid.*, **65,** C-6 (1982).

Technical Note

An Electrochemical Fabrication Method for Platinum Ultramicro Disk Electrodes

Kingo Itaya, Takayuki Abe, and Isamu Uchida

Department of Applied Chemistry, Faculty of Engineering, Tohoku University, Sendai, 980 Japan

Recently there has been considerable interest in electrochemical studies which utilize microelectrodes (1-10). To date, microelectrodes have found applications in areas such as *in vivo* electrochemical studies (3, 4), fast electron transfer reactions (7), and fast, coupled chemical reactions (8). Most investigations on microvoltammetric disk electrodes limit the radius of the electrode to a few tens of micrometers (μm). Commercially available platinum (Pt), gold (Au), and carbon fibers have been widely used (1-10).

The advantages of using microvoltammetric disk electrodes are several: the hemispherical nature of the diffusion field gives a steady-state mass-transfer limited current (13); the reduced area of the electrode results in a diminished charging current (10) and allows the extension of electroanalytical techniques to samples of lower concentration and smaller size (12); and the low ohmic drop incurred with the microelectrodes eliminates the need for a three-electrode system and results in lower system noise (9). The motivation for reducing the disk electrode radius to submicron proportion is that ohmic distortion is virtually eliminated, even in unsupported nonaqueous solvents using a two-electrode system (9).

One technique for fabricating submicron platinum disk electrodes is to use Wollaston wire, a platinum wire inserted into the center of a large silver wire and drawn